

A METHOD FOR THE DESIGN OF AIR-CORE MAGNETS IN TOROIDAL GEOMETRY†

RICHARD K. COOPER,‡ JACK W. BEAL AND V. KELVIN NEIL

University of California, Lawrence Radiation Laboratory, Livermore, California, U.S.A.

A method is developed for the design of air-core magnets wound on toroidal surfaces. With the use of toroidal coordinates, it is possible to find the surface current density on a complete torus that will yield any vector potential of the form $\vec{A} = A_\phi(r, z)\hat{\phi}$ inside the torus, where r , ϕ and z are cylindrical coordinates. The function A_ϕ must satisfy the equation $\nabla^2 A_\phi - A_\phi/r^2 = 0$. The surface current density may be chosen such that no net current flows in the azimuthal (ϕ) direction. The surface current is then replaced by a set of conductors, properly located on the toroidal surface. All conductors carry the same current, which flows in the $+\phi$ -direction in one-half the conductors and in the $-\phi$ -direction in the other half. To construct a magnet of prescribed arc length, the windings can then be connected at the ends to form a continuous current path. Theoretical fields, including the effect of the end windings, are then compared to the measured field of an actual magnet designed by this method.

1. INTRODUCTION

The use of magnets for focusing and steering particle beams is an integral part of the workings of accelerators, storage rings, and beam transport systems. Technology being what it is, such beams are frequently found in round pipes, which are then often bent in circles or arcs thereof. It becomes necessary therefore to design magnets which will produce a given magnetic field in these geometries. It is further desirable on occasion to exclude magnetic materials from the design; such magnets are designated as air-core magnets. This paper treats the problem of the design of air-core magnets which will produce a given azimuthally symmetric magnetic field in the interior of a given torus. The restriction to azimuthal symmetry would seem to limit the treatment to the design of magnets for use with pipes bent into full circles, but this is not the case. The design can be carried out as for a full torus, and then end windings may be emplaced so as to produce a magnet with any desired angular increment (see section on end effects).

2. METHOD

We employ toroidal coordinates to determine the current density on the surface of the given torus

† Work performed jointly under the auspices of the U.S. Atomic Energy Commission and the Advanced Research Projects Agency, Order No. 1377.

‡ Permanent address: California State College, Hayward, Hayward, Calif.

which will produce the desired magnetic field, characterized by the magnetic vector potential \mathbf{A} . We restrict ourselves to azimuthal currents only. That is, the method treats any and all magnetic fields which can be derived from a vector potential of the form $\mathbf{A} = A_\phi(r, z)\hat{\phi}$, (cylindrical coordinates), which satisfies the equation

$$\nabla^2 A_\phi - \frac{A_\phi}{r^2} = 0, \quad (1)$$

in the free space regions inside and outside of the toroidal surface.

The current density determined is not unique, since there exists a current distribution on the toroidal surface which produces no field in the interior. As a practical matter we choose the current density which requires as much positive current as negative current. The current density is translated into discrete conductors carrying equal currents, and for toroidal sectors the positive current conductors are joined to the negative current conductors at the ends of the sector.

3. ANALYSIS

The geometry employed is shown in Fig. 1. The distance from the symmetry (z) axis to the center of the pipe (the major radius) is denoted by R , while the radius of the pipe itself (the minor radius) is denoted by b . We use cylindrical coordinates r , ϕ , z as well as the toroidal coordinates η , θ , ψ as defined in Moon and Spencer.⁽¹⁾ (See Appendix.)

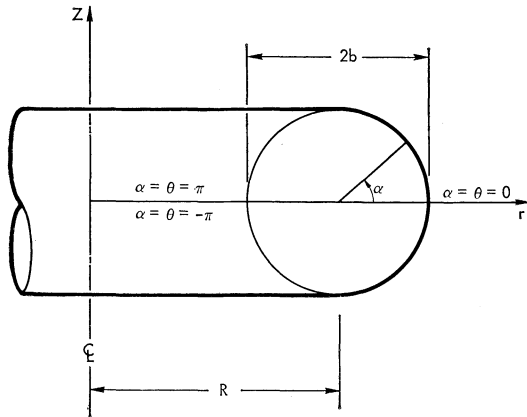


FIG. 1. Toroidal geometry employed.

If we calculate for our pipe the distance $a = \sqrt{(R+b)(R-b)}$, then the toroidal coordinate system with this value for a has the property that the surfaces of constant η are a nested set of toroids, the limiting torus $\eta \rightarrow \infty$ having major radius a and minor radius $\rightarrow 0$. The value of η which gives the pipe surface is $\eta_s = \cosh^{-1} R/b$. The angle θ is related to the angle α given in Fig. 1 by the equation

$$\cos \theta = \frac{(R/b) \cos \alpha + 1}{(R/b) + \cos \alpha},$$

from which it can be seen that at 0 and π the two angles coincide, and for $R/b \gg 1$ the difference between α and θ is very small. The angle ψ is the same as the angle ϕ of our cylindrical coordinate system.

We begin by observing that $A_\phi \equiv A_\psi$ and that Eq. (1) is independent of the coordinate system. When translated into toroidal coordinates, this equation has the solution

$$A_\psi = \sqrt{\xi - \cos \theta} \left[\frac{a_0}{2} Q_{-1/2}^1(\xi) + \sum_{n=1}^{\infty} a_n Q_{n-1/2}^1(\xi) \cos n\theta \right], \quad (2)$$

in which $\xi \equiv \cosh \eta$. This equation is valid⁽²⁾ inside the torus, i.e., for $\eta_s < \eta < \infty$. Outside the torus we have

$$A_\psi = \sqrt{\xi - \cos \theta} \left[\frac{b_0}{2} P_{-1/2}^1(\xi) + \sum_{n=1}^{\infty} b_n P_{n-1/2}^1(\xi) \cos n\theta \right]. \quad (3)$$

The functions of ξ occurring in Eqs. (2) and (3) are associated Legendre functions, which can be defined as follows for $\xi > 1$:

$$P_\nu^m(\xi) = (\xi^2 - 1)^{m/2} \frac{d^m}{d\xi^m} P_\nu(\xi), \quad (4a)$$

where $P_\nu(\xi)$ is given by the Laplace integral representation

$$P_\nu(\xi) = \frac{1}{\pi} \int_0^\pi [\xi + (\xi^2 - 1)^{1/2} \cos \phi]^\nu d\phi. \quad (4b)$$

Likewise we have for the second solutions

$$Q_\nu^m(\xi) = (\xi^2 - 1)^{m/2} \frac{d^m}{d\xi^m} Q_\nu(\xi), \quad (5a)$$

where the integral representation of greatest utility for this work is⁽³⁾ (this time specifically for $\nu = n - \frac{1}{2}$, n an integer)

$$Q_{n-1/2}(\xi) = \frac{1}{\sqrt{2}} \int_0^\pi \frac{\cos n\phi d\phi}{(\xi - \cos \phi)^{1/2}}. \quad (5b)$$

The general procedure then is to take the desired vector potential A_i in the interior of the torus and formally equate it to that given by expression (2). Then by orthogonality of the trigonometric functions we can determine the coefficients a_n as

$$a_n = \frac{1}{\pi Q_{n-1/2}^1(\xi)} \int_{-\pi}^\pi \frac{A_i}{(\xi - \cos \theta)^{1/2}} \cos n\theta d\theta, \quad (6)$$

which is valid for all n . These coefficients are not in fact functions of ξ , and one may choose any value of ξ inside the torus for the evaluation of a_n . A convenient choice is $\xi_s \equiv \cosh \eta_s = R/b$. Knowing the coefficients a_n we can calculate the coefficients b_n by using the fact that A_ψ is continuous at the surface of the torus, i.e., Eqs. (2) and (3) are equivalent at $\xi = \xi_s$. Thus we find that

$$b_n = a_n \frac{Q_{n-1/2}^1(\xi_s)}{P_{n-1/2}^1(\xi_s)}. \quad (7)$$

Having determined these coefficients, the current density K_ψ that produces the given vector potential A_i is found from the discontinuity in the θ -component of the magnetic field \mathbf{B} . That is

$$K_\psi = \frac{1}{\mu_0} (B_{\theta \text{ inside}} - B_{\theta \text{ outside}}). \quad (8)$$

(Rationalized mks units will be used throughout this work.) For azimuthally symmetric fields we have

$$B_\theta = -\frac{(\xi - \cos \theta)^2}{a\sqrt{\xi^2 - 1}} \frac{\partial}{\partial \eta} \left[\frac{\sinh \eta A_\psi}{\cosh \eta - \cos \theta} \right].$$

Only the derivatives of the functions $Q_{n-1/2}^1$ and $P_{n-1/2}^1$ will contribute to the discontinuity in B_θ , since all other factors are continuous. Since

$$\frac{\partial}{\partial \eta} = \sinh \eta \frac{\partial}{\partial \cosh \eta} = \sqrt{\xi^2 - 1} \frac{\partial}{\partial \xi},$$

we have, from Eqs. (2), (3) and (8)

$$K_\psi = \frac{(\xi_s - \cos \theta)^{3/2} \sqrt{\xi_s^2 - 1}}{\mu_0 a} \left\{ \frac{b_0}{2} \frac{dP_{n-1/2}^1}{d\xi} - \frac{a_0}{2} \frac{dQ_{n-1/2}^1}{d\xi} + \sum_{n=1}^{\infty} \left[b_n \frac{dP_{n-1/2}^1}{d\xi} - a_n \frac{dQ_{n-1/2}^1}{d\xi} \right] \cos n\theta \right\}. \quad (9)$$

This expression can be simplified by using Eq. (7) and the Wronskian for these functions, namely

$$P_{n-1/2}^1 \frac{dQ_{n-1/2}^1}{d\xi} - Q_{n-1/2}^1 \frac{dP_{n-1/2}^1}{d\xi} = \frac{n^2 - \frac{1}{4}}{\xi^2 - 1}. \quad (10)$$

The expression for the current density becomes

$$K_\psi = \frac{(\xi_s - \cos \theta)^{3/2}}{\mu_0 a \sqrt{\xi_s^2 - 1}} \cdot \left\{ \frac{a_0}{8P_{-1/2}^1(\xi_s)} - \sum_{n=1}^{\infty} \frac{a_n(n^2 - \frac{1}{4})}{P_{n-1/2}^1(\xi_s)} \cos n\theta \right\}, \quad (11)$$

where the coefficients a_n are given by Eq. (6). Equation (11) gives the current density as a function of the angle α through the use of the relation between θ and α , since the number of amperes per unit length is merely a number, irrespective of coordinate system. That is, $K(\alpha) = K_\psi(\theta(\alpha))$. In the next two sections, Eq. (11) is evaluated analytically for the distribution which produces no field in the interior of the torus, and then for the distribution which produces a uniform field in the z -direction in the interior.

4. THE CURRENT DISTRIBUTION WHICH PRODUCES NO INTERIOR FIELD

The vector field $\mathbf{A} = (\Phi/r) \hat{\phi}$ in cylindrical coordinates has zero curl, and any current distribution

which produces this vector field is a distribution that generates no magnetic field. Of course we are speaking of finite regions of space over which these fields exist, and in particular we want to know what current distribution on the surface of a torus that will yield the vector potential specified in the interior. This current distribution is given by Eq. (11), with the expansion coefficients a_n found from Eq. (6). We note that $r = a(\xi^2 - 1)^{1/2}/(\xi - \cos \theta)$, and obtain

$$a_n = \frac{\Phi}{\pi a Q_{n-1/2}^1(\xi)} \frac{1}{\sqrt{\xi^2 - 1}} \int_{-\pi}^{\pi} \frac{(\xi - \cos \theta) \cos n\theta d\theta}{(\xi - \cos \theta)^{1/2}},$$

$$= \frac{\Phi}{\pi a \sqrt{\xi^2 - 1}} \frac{2\sqrt{2}}{Q_{n-1/2}^1(\xi)} \cdot [\xi Q_{n-1/2}^1(\xi) - \frac{1}{2} Q_{n+1/2}^1 - \frac{1}{2} Q_{n-3/2}^1], \quad (12)$$

in which we have also used Eq. (5b).

The ξ -dependent terms in the denominator can be rewritten as

$$\sqrt{\xi^2 - 1} Q_{n-1/2}^1(\xi) = (\xi^2 - 1) \frac{dQ_{n-1/2}^1}{d\xi} = (n - \frac{1}{2}) [\xi Q_{n-1/2}^1 - Q_{n-3/2}^1], \quad (13)$$

which follows from

$$(\xi^2 - 1) \frac{dQ_\nu}{d\xi} = \nu(\xi Q_\nu - Q_{\nu-1}). \quad (14)$$

In addition, use of the recurrence relation⁽⁴⁾

$$(\nu + 1)Q_{\nu+1} = (2\nu + 1)\xi Q_\nu - \nu Q_{\nu-1}, \quad (15)$$

with $\nu = n - \frac{1}{2}$ yields

$$\xi Q_{n-1/2} - \frac{1}{2}(Q_{n+1/2} + Q_{n-3/2}) = (\xi Q_{n-1/2} - Q_{n-3/2}) / (2n + 1). \quad (16)$$

Inserting Eqs. (13) and (16) into Eq. (12), we have for the expansion coefficients

$$a_n = \frac{\Phi}{\pi a} \frac{2\sqrt{2}}{(n - \frac{1}{2})(2n + 1)} = \frac{\Phi\sqrt{2}}{\pi a(n^2 - \frac{1}{4})}. \quad (17)$$

From Eq. (11) we find the current density producing no field in the interior of the torus to be given by

$$K_{\text{null}}(\theta) = -\frac{(\xi_s - \cos \theta)^{3/2} \Phi \sqrt{2}}{\mu_0 a \sqrt{\xi_s^2 - 1} \pi a} \cdot \left\{ \frac{1}{2P_{-1/2}^1(\xi_s)} + \sum_{n=1}^{\infty} \frac{\cos n\theta}{P_{n-1/2}^1(\xi_s)} \right\}, \quad (18)$$

where it should be recalled that $\xi_s = R/b$.

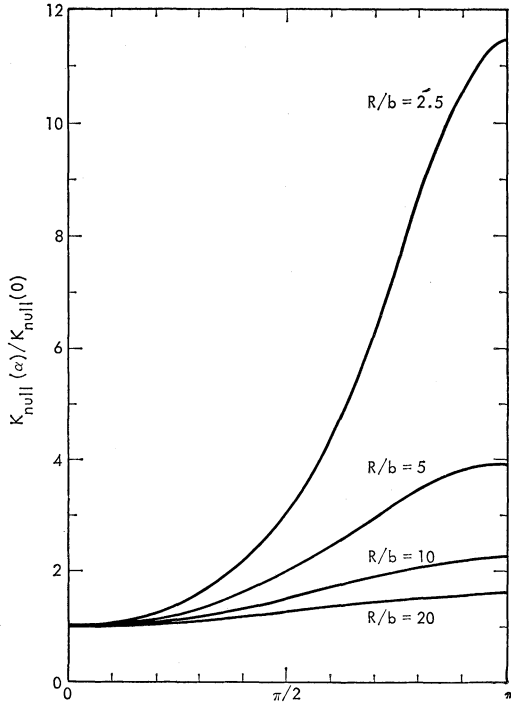


FIG. 2. The surface current density K_{null} that results in a vector potential $\propto 1/r$ inside the torus as a function of α for various values of R/b . The curves are normalized such that $K_{\text{null}}(0) = 1.0$.

Since Φ was an arbitrary constant, we can choose it to be $-\mu_0 \pi(R^2 - b^2)/\sqrt{2}$, thereby leaving an expression for the current distribution (with a dimensional constant of magnitude unity implied) which displays the essential dependence of the distribution on the geometry, namely the single parameter R/b .

$$K_{\text{null}}(\theta) = (R/b - \cos \theta)^{3/2}$$

$$\cdot \left\{ \frac{1}{2P_{-1/2}^1(R/b)} + \sum_{n=1}^{\infty} \frac{\cos n\theta}{P_{n-1/2}^1(R/b)} \right\}. \quad (19)$$

This distribution was evaluated numerically for various values of R/b and is shown in Fig. 2. For $R/b \rightarrow \infty$, the distribution approaches a constant and as R/b decreases, the distribution becomes increasingly non-uniform.

5. THE CURRENT DISTRIBUTION WHICH PRODUCES A UNIFORM FIELD

The vector field $\mathbf{A} = \frac{1}{2}Br\hat{\phi}$ has a curl given by $B\hat{z}$ (cylindrical coordinates). Thus if we wish to

produce a uniform field in the z -direction in the interior of a torus, we must find the current distribution which produces $A_\phi = \frac{1}{2}Br$. This entails calculating the coefficients (recall that $r = a(\xi^2 - 1)^{1/2}/(\xi - \cos \theta)$)

$$a_n = \frac{Ba\sqrt{\xi^2 - 1}}{2\pi Q_{n-1/2}^1(\xi)} \int_{-\pi}^{\pi} \frac{\cos n\theta d\theta}{(\xi - \cos \theta)^{3/2}}.$$

We may evaluate the integral as follows:

$$\begin{aligned} \int_{-\pi}^{\pi} \frac{\cos n\theta d\theta}{(\xi - \cos \theta)^{3/2}} &= -2 \frac{\partial}{\partial \xi} \int_{-\pi}^{\pi} \frac{\cos n\theta d\theta}{(\xi - \cos \theta)^{1/2}} \\ &= -2 \frac{\partial}{\partial \xi} 2\sqrt{2} Q_{n-1/2}(\xi) \\ &= -4\sqrt{2} \frac{Q_{n-1/2}^1(\xi)}{\sqrt{\xi^2 - 1}} \end{aligned}$$

the last two equalities following from Eqs. (5a) and (5b). Thus the expansion coefficients are

$$a_n = -Ba2\sqrt{2}/\pi. \quad (20)$$

Thus the current density which produces a uniform field of strength B in the z -direction is

$$\begin{aligned} K_{\text{uniform}}(\theta) &= \frac{2\sqrt{2}B(\xi_s - \cos \theta)^{3/2}}{\mu_0 \pi \sqrt{\xi_s^2 - 1}} \left\{ \frac{-1}{8P_{-1/2}^1(\xi_s)} \right. \\ &\quad \left. + \sum_{n=1}^{\infty} \frac{(n^2 - \frac{1}{4}) \cos n\theta}{P_{n-1/2}^1(\xi_s)} \right\}. \quad (21) \end{aligned}$$

It should be noted that this distribution is only a function of $\xi_s \equiv R/b$. That is, the distribution is independent of the absolute size of the torus. The total current required to produce the desired field will be a linear function of the size, i.e., will be proportional to b .

6. PRACTICAL CONSIDERATIONS

An integration of the current density of Eq. (21) over the surface of the torus will give the total current required to produce the uniform magnetic field described by the vector potential $\mathbf{A} = \frac{1}{2}Br\hat{\phi}$. Given that the metric coefficient for θ is $h_\theta =$

$a/(\xi - \cos \theta)$, the current is found from the expression

$$I_{\text{uniform}} = \frac{2\sqrt{2}B}{\mu_0 \pi} a \int_{-\pi}^{\pi} (\xi_s - \cos \theta)^{1/2} \cdot \left[-\frac{1}{8P_{-1/2}^1(\xi_s)} + \sum_{n=1}^{\infty} \frac{(n^2 - \frac{1}{4}) \cos n\theta}{P_{n-1/2}^1(\xi_s)} \right] d\theta.$$

The manipulations following Eq. (12) can be summarized by the equation

$$\int_{-\pi}^{\pi} (\xi - \cos \theta)^{1/2} \cos n\theta d\theta = \frac{\sqrt{2}}{(n^2 - \frac{1}{4})} \sqrt{\xi^2 - 1} Q_{n-1/2}^1(\xi). \quad (22)$$

Substituting this relation into the previous expressions gives

$$I_{\text{uniform}} = \frac{4Ba}{\mu_0 \pi} \left[\frac{1}{2} \frac{Q_{-1/2}^1(\xi_s)}{P_{-1/2}^1(\xi_s)} + \sum_{n=1}^{\infty} \frac{Q_{n-1/2}^1(\xi_s)}{P_{n-1/2}^1(\xi_s)} \right]. \quad (23)$$

Similarly, the evaluation of the total current described by $K_{\text{null}}(\theta)$ is

$$I_{\text{null}} = a \int_{-\pi}^{\pi} (\xi_s - \cos \theta)^{1/2} \cdot \left\{ \frac{1}{2P_{-1/2}^1(\xi_s)} + \sum_{n=1}^{\infty} \frac{\cos n\theta}{P_{n-1/2}^1(\xi_s)} \right\} d\theta = a\sqrt{2} \sqrt{\xi_s^2 - 1} \cdot \left\{ -2 \frac{Q_{-1/2}^1(\xi_s)}{P_{-1/2}^1(\xi_s)} + \sum_{n=1}^{\infty} \frac{1}{(n^2 - \frac{1}{4})} \frac{Q_{n-1/2}^1(\xi_s)}{P_{n-1/2}^1(\xi_s)} \right\}. \quad (24)$$

Multiplication of $K_{\text{null}}(\theta)$ by a constant k merely multiplies this latter current by k . As a practical case, we would like the total integrated current to be zero, so that positive and negative current densities are required. Thus the wires carrying positive current can be bent back to provide the negative current. This condition can be satisfied if we use as our current density $K(\theta) = K_{\text{uniform}}(\theta) -$

$kK_{\text{null}}(\theta)$, where the constant k is given by

$$k = \frac{I_{\text{uniform}}}{I_{\text{null}}} = \frac{2\sqrt{2}B}{\mu_0 \pi \sqrt{(R/b)^2 - 1}} \cdot \left[\frac{1}{2} \frac{Q_{-1/2}^1(R/b)}{P_{-1/2}^1(R/b)} + \sum_{n=1}^{\infty} \frac{Q_{n-1/2}^1(R/b)}{P_{n-1/2}^1(R/b)} \right] \cdot \left[-2 \frac{Q_{-1/2}^1(R/b)}{P_{-1/2}^1(R/b)} + \sum_{n=1}^{\infty} \frac{1}{(n^2 - \frac{1}{4})} \frac{Q_{n-1/2}^1(R/b)}{P_{n-1/2}^1(R/b)} \right]^{-1}. \quad (25)$$

If the ratio of the two bracketed quantities is denoted by $T(R/b)$, then the current density actually used in the design is given by

$$K(\theta) = \frac{2\sqrt{2}B(R/b - \cos \theta)^{3/2}}{\mu_0 \pi \sqrt{(R/b)^2 - 1}} \cdot \left\{ \frac{-(1+4T)}{8P_{-1/2}^1(R/b)} + \sum_{n=1}^{\infty} \frac{\cos n\theta (n^2 - \frac{1}{4} - T)}{P_{n-1/2}^1(R/b)} \right\}. \quad (26)$$

This expression has been evaluated for various values of R/b ; the results are shown in Fig. 3. Table I gives the values of T for various values of R/b .⁽⁵⁾

TABLE I
Values of T for various values of R/b

R/b	T
2.5	-0.20072
5.0	-0.23217
10.0	-0.24396
20.0	-0.24807

One cannot, of course, actually achieve the current density given by Eq. (26) with a finite number of current-carrying conductors. It is necessary therefore to devise an approximation to the desired density which can be implemented by actual hardware. A first step towards establishing a practical current distribution can be taken by dividing the current distribution into N segments (if N conductors are to be employed), each of which contains the same current. If each segment of the continuous current distribution is then replaced by a conductor, carrying the same current and located

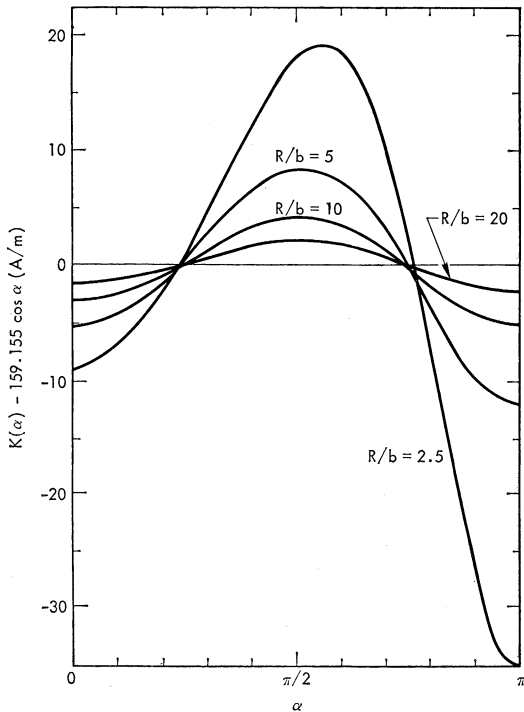


FIG. 3. Plots of $K(\alpha) - 159.155 \cos \alpha$, where $K(\alpha)$ is the distribution that yields a uniform $B_z = 1$ gauss and has zero net current (Eq. (26)). The surface current distribution $159.155 \cos \alpha$ yields a uniform $B_z = 1$ gauss in a straight pipe.

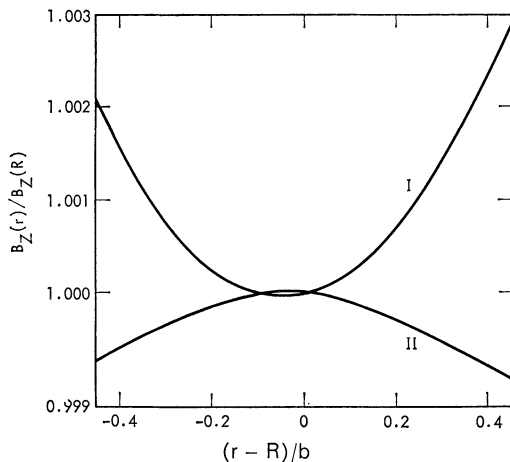


FIG. 4. Relative field strength $B_z(r)/B_z(R)$ vs $(r-R)/b$ in the plane $z=0$. Curve I results from locating the conductors in the center of each angular segment, while curve II results from locating the conductors at the 'center of gravity' of each angular segment.

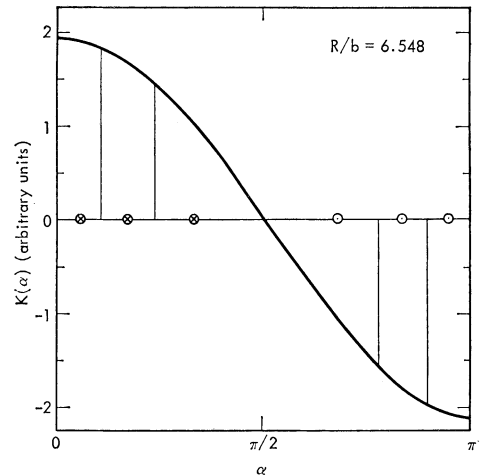


FIG. 5. Division of the surface current distribution into segments carrying equal current. The vertical lines are the ends of the segments, and the circles indicate the location of conductors used to simulate the surface distribution.

in the middle of the segment, we will have an actual distribution that resembles the desired distribution. The results of such a procedure are displayed for a magnet with $R = 2.29$ m, $b = 0.35$ m in Fig. 4, in which the density of Eq. (26) was approximated by a total of 40 conductors. Note that the scale on the abscissa is highly magnified. An improvement of the resulting field can be obtained if instead of placing the conductors in the middle of the segments they are placed at the 'center of gravity' of the segment, i.e., at

$$\alpha_p = \frac{1}{I} \int_{\alpha_0}^{\alpha_1} K(\alpha) d\alpha,$$

where I is the current in one segment and α_0 and α_1 are the angles delimiting the ends of the segment. Such a division is shown schematically in Fig. 5 for $N = 12$. The results of shifting the conductors to these locations are also shown in Fig. 4. The total variation of the field has been reduced from the previous placement, and the gradient of the field has changed sign. Presumably the best placement for the conductors lies somewhere in between the two choices given above.

7. END EFFECTS

There is a limited demand for magnets which will bend or focus a charged particle beam in a full

circle. More practical designs must allow for circular arcs, with the resultant necessity of considering the ends of the arcs. It is at the ends that we have the opportunity to derive maximum benefit from having chosen the total current to be zero, for it is here that the positive current-carrying conductors can be bent back to form the negative current-carrying conductors. End windings are shown schematically in Fig. 6. End windings of an

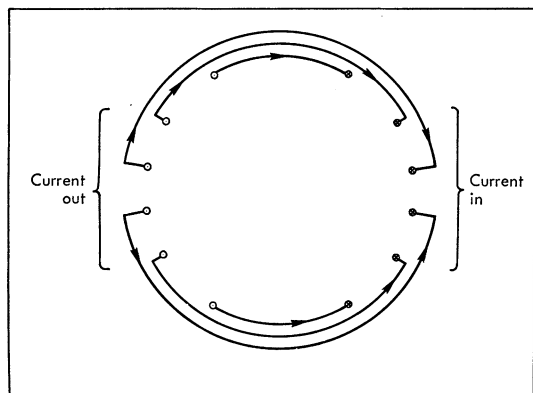


FIG. 6. Schematic drawing of the end windings of a 12-conductor array.

actual magnet can be seen in Fig. 8b. The fields produced by the end windings may be studied analytically by representing their effect as due to a circular conductor of radius b carrying a current varying with the angle:

$$I(\alpha) = -b \int_0^\alpha K(\alpha) d\alpha.$$

Such studies⁽⁶⁾ based on windings on the surface of a right circular cylinder indicate that the end windings have a salutary effect in that they sharpen the cutoff of fields outside the magnet over what would result if the currents could somehow be caused to start and terminate at the end without additional windings. The calculated fields of a finite length bending magnet of toroidal design are shown in Fig. 7 as a function of distance from the center of the magnet along the design center ($r = R$, $z = 0$ in the toroidal section, axis of the pipe in the straight section as shown in Fig. 7). The magnet has $R = 2.29$ m, $b = 0.35$ m, and an effective length of 1.8 m. Also shown in Fig. 7 are

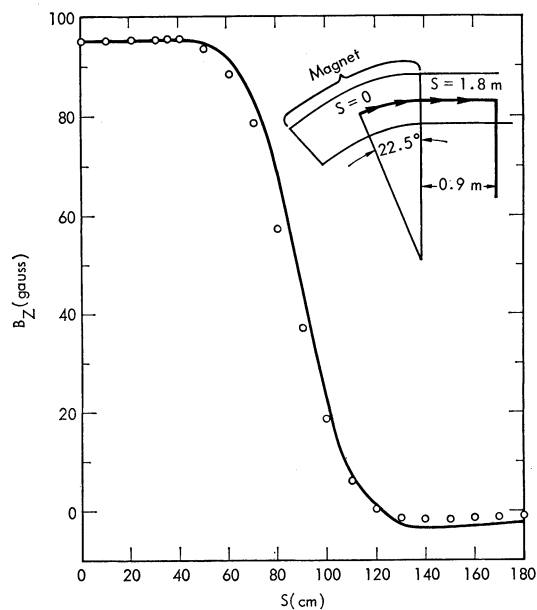


FIG. 7. Calculated field strength B_z (solid line) for a magnet with $R = 2.29$ m, $b = 0.35$ m, with an effective length of 1.8 m. The field is calculated along the path shown in the insert. The circled points represent measured values of the field for an actual magnet that is 10 cm shorter than that for which the curve was calculated.

experimentally measured values of the field produced by an actual magnet, which is shown in Fig. 8. For engineering reasons the effective length of the actual magnet is 1.7 m.

8. QUADRUPOLE FOCUSING FIELDS IN TOROIDAL GEOMETRY

Conventional focusing magnets produce fields which increase in strength linearly from the axis. That is, if the y -axis be chosen as the direction of travel of the beam, the magnetic field will be given by

$$\mathbf{B} = B_0(z\hat{x} + x\hat{z})/R,$$

where R is a length characterizing the field gradient ($= B_0/R$). These quadrupole fields are produced by a vector potential

$$\mathbf{A} = \hat{y}B_0(x^2 - z^2)/2R.$$

In a toroidal geometry the simplest vector potential that satisfies $\nabla^2 A_\phi - A_\phi/r^2 = 0$, and produces fields closely approximating those of a conventional

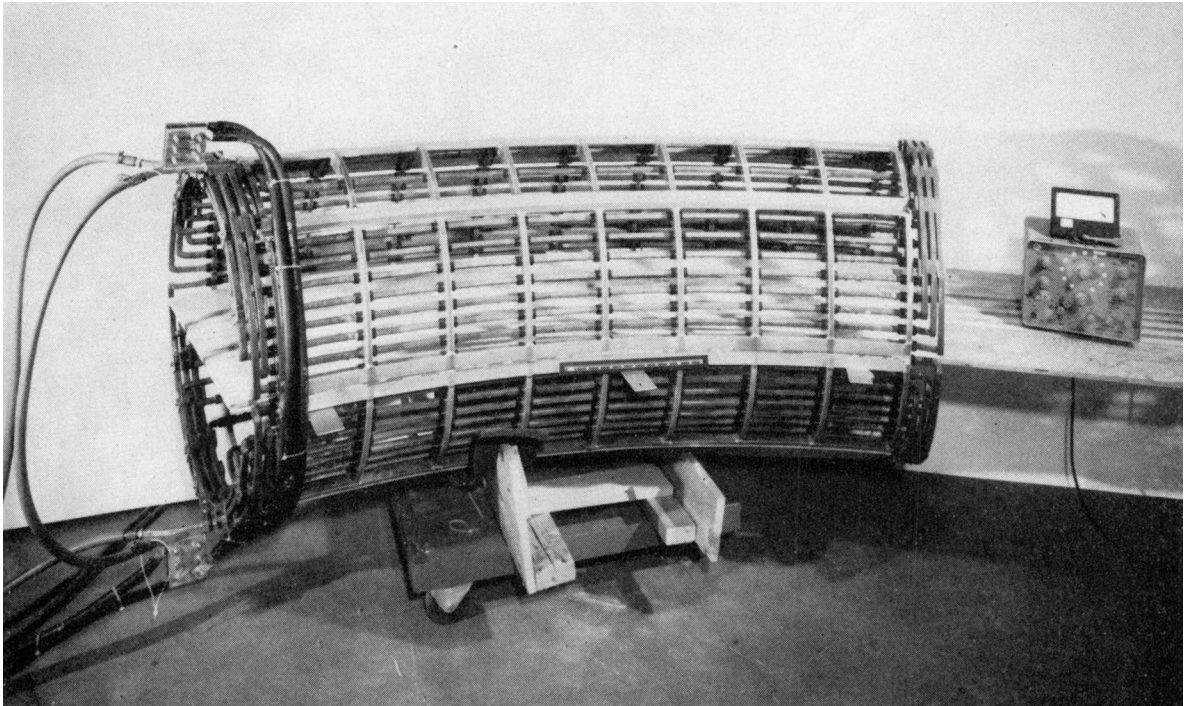


FIG. 8a. Photograph of a magnet with $R = 2.29$ m, $b = 0.35$ m with an effective length of 1.7 m.

quadrupole has been found to be (cylindrical coordinates)

$$\mathbf{A} = \hat{\phi} \frac{B_0}{2r} \left[r^2 \left(\ln \frac{r}{R} - \frac{1}{2} \right) - z^2 \right]. \quad (28)$$

The field produced by this potential is

$$\mathbf{B} = B_0 \left[\hat{r} \frac{z}{r} + \hat{z} \ln \frac{r}{R} \right]. \quad (29)$$

If we let $r = R + x$ and retain only first order terms in displacement from the center of the torus, the magnetic field given by Eq. (29) is seen to be identical to that given by Eq. (27), where now R is the major radius of the torus.

To find the current density which produces the vector potential given by (28) is then simply a matter of evaluating the integrals in Eq. (6) with Eq. (28) determining the integrand. While it is in principle possible to do these integrals analytically, we decided that numerical evaluation would be easier, and since the rest of the design procedure necessitated use of the computer, the computer program named COPOUT was written.

9. THE COPOUT PROGRAM

This computer program takes an arbitrary $A_\phi(r, z)$ specified by a card in the program and numerically evaluates the integrals in Eq. (6) by Filon's method.⁽⁷⁾ The associated Legendre functions are then generated by numerical evaluation of the Laplace integral representations

$$P_{n-1/2}^1(z) = \frac{(n+1/2)}{\pi} \int_0^\pi (z + (z^2-1)^{1/2} \cos \phi)^{n-1/2} \cos \phi \, d\phi,$$

and

$$Q_{n-1/2}^1(z) = -\frac{(z^2-1)^{1/2}}{2\sqrt{2}} \int_0^\pi \frac{\cos n\phi \, d\phi}{(z - \cos \phi)^{3/2}}.$$

Again, for $n = 0$ and 1, Filon's method is used. The recurrence relation⁽⁸⁾

$$(n-m)U_n^m(x) = (2n-1)xU_{n-1}^m(x) - (n+m-1)U_{n-2}^m(x),$$

in which U stands for either P or Q is then used

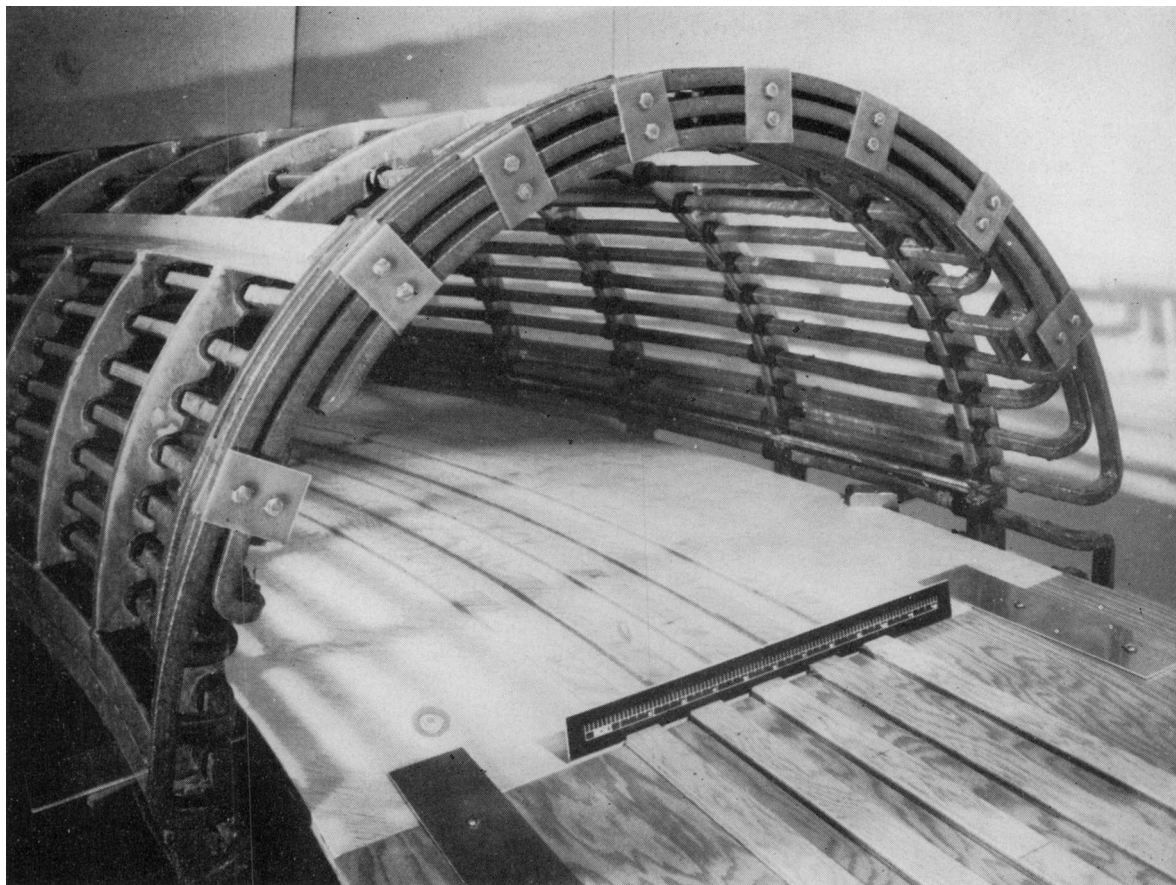


FIG 8b. Details of end windings of magnet shown in Fig. 8a.

to obtain the rest of the P 's. The Q 's are generated by Miller's method⁽⁹⁾ which employs backward recurrence and needs a value of $Q_{n-1/2}^1$ for only one n value, chosen to be $n = 0$.

The expression, Eq. (11), for the current density is then evaluated by truncating the series after a finite number of terms.⁽¹⁰⁾ The null current density is also evaluated and the factor k in Eq. (25) is calculated by taking the ratio of the numerically integrated total current $I_{\text{desired field}}$ and I_{null} . The resulting distribution K_{actual} is then represented by conductors according to the scheme outlined in Section VI, with NCOND, the number of conductors to represent the distribution, being an input parameter of the program.

A listing of the program, written in FORTRAN, is available on request.⁽¹¹⁾

APPENDIX—TOROIDAL COORDINATES⁽¹⁾

The toroidal coordinate system used throughout the paper can be defined through the relations

$$x = \frac{a \sinh \eta \cos \psi}{\cosh \eta - \cos \theta},$$

$$y = \frac{a \sinh \eta \sin \psi}{\cosh \eta - \cos \theta},$$

$$z = \frac{a \sin \theta}{\cosh \eta - \cos \theta},$$

in which $0 \leq \eta < \infty$, $-\pi < \theta \leq \pi$, $0 \leq \psi < 2\pi$.

The coordinate surfaces are given by toroids, ($\eta = \text{const}$)

$$x^2 + y^2 + z^2 + a^2 = 2a(x^2 + y^2)^{1/2} \coth \eta,$$

spherical bowls ($\theta = \text{const}$)

$$x^2 + y^2 + (z - a \cot \theta)^2 = \frac{a^2}{\sin^2 \theta},$$

and half planes ($\psi = \text{const}$)

$$\tan \psi = y/x.$$

In terms of these coordinates the Laplacian is

$$\begin{aligned} \nabla^2 \phi &= \frac{(\cosh \eta - \cos \theta)^3}{a^2 \sinh \eta} \\ &\cdot \left\{ \frac{\partial}{\partial \eta} \left(\frac{\sinh \eta}{\cosh \eta - \cos \theta} \frac{\partial \phi}{\partial \eta} \right) \right. \\ &\quad \left. + \sinh \eta \frac{\partial}{\partial \theta} \left(\frac{1}{\cosh \eta - \cos \theta} \frac{\partial \phi}{\partial \theta} \right) \right\} \\ &+ \frac{(\cosh \eta - \cos \theta)^2 \partial^2 \phi}{a^2 \sinh^2 \eta \partial \psi^2}. \end{aligned}$$

The solutions of $\nabla^2 \phi = 0$ are

$$\begin{aligned} \phi &= (\cosh \eta - \cos \theta)^{1/2} \left\{ P_{n-1/2}^m(\cosh \eta) \right\} \\ &\quad \left\{ Q_{n-1/2}^m(\cosh \eta) \right\} \\ &\cdot \left\{ \begin{matrix} \sin n\theta \\ \cos n\theta \end{matrix} \right\} \cdot \left\{ \begin{matrix} \sin m\psi \\ \cos m\psi \end{matrix} \right\}, \end{aligned}$$

where the braces mean an appropriate linear combination of the functions displayed therein. Notice that for this solution, the last term of the Laplacian expression becomes simply $-m^2 \phi / r^2$, where $r = (x^2 + y^2)^{1/2} = a \sinh \eta / (\cosh \eta - \cos \theta)$ is the radius in cylindrical coordinates. Thus if we have a function which is independent of ψ and satisfies $\nabla^2 A - A/r^2 = 0$ we see that the solution is

$$A = (\cosh \eta - \cos \theta)^{1/2} \left\{ P_{n-1/2}^1(\cosh \eta) \right\} \cdot \left\{ \begin{matrix} \sin n\theta \\ \cos n\theta \end{matrix} \right\}.$$

Finally, in these coordinates the curl of a vector is given by

$$\text{curl } \mathbf{A} = \frac{(\cosh \eta - \cos \theta)^2}{a \sinh \eta} \begin{vmatrix} \hat{\eta} & \hat{\theta} & \hat{\psi} \sinh \eta \\ \frac{\partial}{\partial \eta} & \frac{\partial}{\partial \theta} & \frac{\partial}{\partial \psi} \\ A_\eta & A_\theta & A_\psi \sinh \eta \end{vmatrix}.$$

$$\begin{matrix} \cosh \eta - \cos \theta & \cosh \eta - \cos \theta & \cosh \eta - \cos \theta \end{matrix}$$

REFERENCES

1. P. Moon and D. E. Spencer, *Field Theory Handbook*, Springer Verlag, 112 (1961).
2. It has been assumed here that A_ϕ is an even function of z , i.e., that B_r is an odd function of z . If A_ϕ should contain odd terms in z , then the solution of Eq. (2) should contain $\sin n\theta$ terms as well. For practical applications to accelerators, the form used here is the one most frequently encountered.
3. P. M. Morse and H. Feshbach, *Methods of Theoretical Physics*, McGraw-Hill, 1304 (1953).
4. E. T. Whittaker and G. N. Watson, *Modern Analysis*, Cambridge University Press, 318 (1946).
5. For $R/b \geq 2.5$, four terms in each series will yield a value of T good to at least four significant figures.
6. Lloyd Smith, private communication.
7. M. Abramowitz and I. A. Stegun, eds., *Handbook of Mathematical Functions*, National Bureau of Standards Applied Mathematics Series No. 55, U.S. Govt. Printing Office, 890 (1964).
8. National Bureau of Standards, *Table of Associated Legendre Functions*, Columbia University Press, p. xvi (1945).
9. M. Abramowitz and I. A. Stegun, op. cit., p. XIII.
10. We have used terms up to $n=12$. The P 's increase exponentially with n , so that for $R/b = 2.5$, the ratio $P_{-1/2}^1 / P_{23/2}^1 = 1.17 \times 10^{-9}$. For larger values of R/b the ratio is even smaller. The Q 's decrease exponentially with n . The tables referred to in footnote 8 should prove adequate for many designs.
11. Richard K. Cooper, 'Description of the Computer Program COPOUT,' UCID-30014, May 14, 1971.

Received 7 June 1971